Multimedia Tools and Applications (2021) 80:33573–33591
https://doi.org/10.1007/s11042-021-11402-0

An optimal feature enriched region of interest (ROI) extraction for periocular biometric system

Punam Kumari[1] · **Seeja K.R**[1]

Received: 24 September 2020 / Revised: 26 January 2021 / Accepted: 2 August 2021 /
Published online: 20 August 2021

Abstract
With the onset of COVID-19 pandemic, wearing of face mask became essential and the face occlusion created by the masks deteriorated the performance of the face biometric systems. In this situation, the use of periocular region (region around the eye) as a biometric trait for authentication is gaining attention since it is the most visible region when masks are used. One important issue in periocular biometrics is the identification of an optimal size periocular ROI which contains enough features for authentication. The state of the art ROI extraction algorithms use fixed size rectangular ROI calculated based on some reference points like center of the iris or centre of the eye without considering the shape of the periocular region of an individual. This paper proposes a novel approach to extract optimum size periocular ROIs of two different shapes (polygon and rectangular) by using five reference points (inner and outer canthus points, two end points and the midpoint of eyebrow) in order to accommodate the complete shape of the periocular region of an individual. The performance analysis on UBIPr database using CNN models validated the fact that both the proposed ROIs contain enough information to identify a person wearing face mask.

Keywords Periocular biometrics · Region of interest · Convolutional neural network · COVID-19

1 Introduction

Uniquely identifying individual in this era of pandemic on day to day basis is a challenge in the biometric world. Primary reason is the necessity to use face mask to protect from the spreading of corona virus. Finger print biometric systems are also not considered as a safe option due to the fear of corona virus spread [9]. One of the solutions may be to use

✉ Seeja K.R
seeja@igdtuw.ac.in

Punam Kumari
punam_taurus@hotmail.com

[1] Department of Computer Science & Engineering, Indira Gandhi Delhi Technical University for Women, Delhi, India

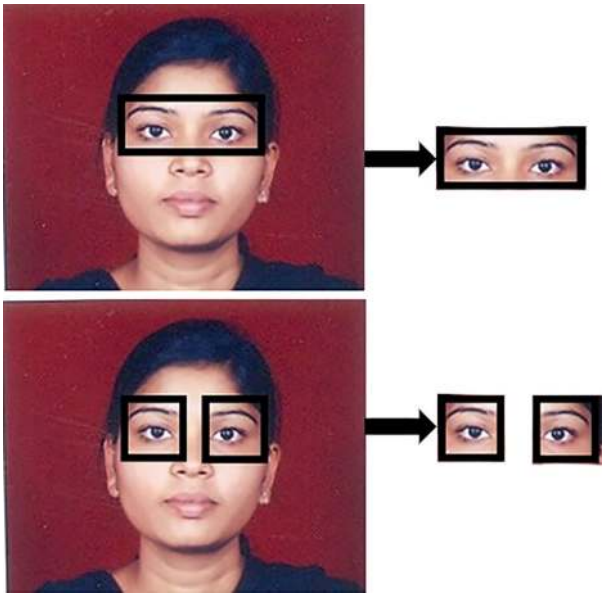

Fig. 1 Examples of periocular region

eye or iris biometrics but it needs a lot of user cooperation. Under this situation, periocular region as a biometric trait is receiving popularity [1] since it is contact less and the performance is least affected by the face mask. The term periocular refers to the periphery of eyes which contains eye, eyebrow and pre-eye orbital region as shown in Fig. 1.

Unlike other biometric traits such as iris, face and fingerprints, the area of periocular region is not defined in literature. Performance of a periocular biometric system strongly depends on the area of the periocular region. It is found that large size periocular region may provide high accuracy but can take more execution time whereas small size periocular region may provide comparable recognition accuracy with less execution time. This is due to the fact that large size ROI obviously contains a greater number of features as compared to small size ROI. But the question is, are all of the features extracted from large size ROI actually worthy to improve recognition accuracy of the system? Or, one should try to extract an optimum size ROI to get enough number of features while maintaining the recognition accuracy of the system. The requirement of small size ROI is also important in the situation of COVID-19 pandemic since a large region of the face is generally covered with the face mask as shown in Fig. 2.

Motivating from the above facts, this research proposes two novel methods to extract two different optimum sized periocular regions of interest, which include the critical components

Fig. 2 Example images when face is covered with face mask

such as eye shape, eye socket, canthus points etc. for authentication when most part of the face is covered with the face mask. The significant contributions of this research are:

1. Proposed a novel methods to extract ROIs of two different shapes: 1) polygon and 2) rectangular shape from periocular region images which contain sufficient features for recognition when subjects are wearing face masks.
2. Demonstrated that the extracted polygon shaped and rectangular shaped ROIs using the proposed methods are capable enough to obtain a better recognition accuracy as compared to the state-of-the-art rectangular ROIs.

The proposed methods can be implemented to create a highly robust contact less biometric authentication system suitable for this pandemic situation.

2 Literature review

In the effort to mitigate the spreading speed of corona virus, face masks are playing a major role. But, use of face mask covered most of the face area which can be a major hurdle for face recognition in person authentication. Damer et al. [7] study the effect of wearing face mask on face recognition systems and found significant drop in recognition accuracy when subject is wearing face mask. Finger print authentication can be a solution but it requires to touch the surface of the scanner which may increase the possibility of contamination and spread of any infectious diseases [18]. Hence in this critical scenario of COVID 19, this solution cannot be acceptable when every automated system needs to work on contact less approach. Iris or sclera matching to identify an individual cannot be considered as a good solution because it requires a lot of user cooperation. In this scenario, use of periocular region as a biometric trait for person authentication is a good solution. The reasons are 1) Periocular region based biometric system works on contact less approach 2) It requires very low user cooperation 3) Since area and shape of periocular region is not defined, system can consider any shape of ROI which has enough feature for person authentication.

The pioneer work to contemplate the adequacy of periocular region as a compelling biometric trait was performed by Park et al. [19]. Subsequently, several works were published to prove the utility of periocular region as supporting feature to iris [4], its usefulness in soft biometric classification [6] and in smart phone authentication [25]. In spite of the popularity of periocular region as a reliable and contact less biometric trait, the primary challenge for the researcher's community is its undefined size and this problem became more complex when most of the face area is covered with face mask. In literature, various strategies and reference points were considered by the researchers to segment the region of interest from periocular images for matching. Park et al. [21] considered the iris center as reference point and extract a rectangular ROI region with dimension of $(6 \times Riris) \times (4 \times Riris)$ where Riris denotes the radius of iris whereas Ahmed et al. [2] extracted a rectangular ROI region with dimension of $(4 \times Diris) \times (3 \times Diris)$ where Diris denotes the diameter of iris with iris center as reference point. Center of iris is performing well as reference points but these methods were not applicable when eyes were partially or fully closed, face of the subject is tilted and if gaze angle is not frontal.

In order to handle the problem of gaze angle, Mahalingam et al. [15] used eye center instead of iris center as reference points. This method was working well, but again, it

was not applicable on the subjects with tilted head/ face or with partially open eyes. To solve this problem, some investigators proposed to use eye corners as reference points [6, 11]. The reason is, eye corner also known as Canthus points are least effected by partial open eyes or tilted face. In another approach found in literature proposed by Dong and Woodard [8], Le et al. [13] and Nguyen et al. [16], instead of using any reference points they consider critical components of periocular region such as shape of eye brow itself as the region of interest for matching. Proenca et al. [22] proposed a unique method to extract ROI by considering center of mass of cornea as reference points and claimed that their proposed method is least sensitive to gaze angle of eyes.

Most of the approaches in literature provided a fixed size rectangular region of interest. Considering this fact, Bakshi et al. [3] proposed a human anthropometric based method and implemented an approach to extract dynamic region of interest. They considered width of eyebrow, width of face, height of face, area of face and distance between eyebrow and eye center of individual to create and extract a rectangular region of interest. Here the area of ROI can be varied based on the above parameters.

Considering the popularity of deep learning concepts, Proenca and Neves [23] implemented a CNN model and found that components inside ocular globe (such as iris and sclera) does not play a critical role in improving the performance of periocular system. Instead, they may be the cause of degradation in performance. For supporting this disruptive hypothesis, they provided some supporting facts such as 1) effect of corneal reflections in iris and sclera, 2) components in ocular globe are subject to motion because of body or head movement and 3) partial occlusion of iris and sclera because of unknown movements of eyelashes or eyelids. On the contrary, Zhao and Kumar [27] implemented an attention mechanism-based CNN model to make focus on some of the important components of periocular region such as eye shape and eyebrow. The key assumption of their work was that, there may be some critical components in periocular region which required more attention and may provide more discriminative features at the time of matching.

After rigorous study of various state of the art methods implemented in the domain of periocular biometrics, it is found that none of the researchers analyzed the efficiency of periocular biometric system when a large part of face is occluded with the face mask and what solution can considered to improve the performance of the system in this scenario.

Considering the above facts and current pandemic situation, this research proposes two algorithms to extract optimal feature enriched regions of two different shapes (polygon and rectangle) from the visible periocular area. This research also considered the importance of critical components such as eyebrow, shape of eye, eye socket and canthus points and included them in the proposed polygon and rectangular shaped ROIs.

3 Materials and methods

3.1 Database used

For the evaluation of proposed work, raw input images from publicly available UBIPr periocular database created by Padole and Proenca [20] is used. This database contains total 10252 images represented in RGB color space in .bmp format. Images were captured using CANON EOS 5D digital Camera in highly controlled lab conditions and setups such as four meter to eight meter in steps of one meter distance variation, different illumination, frontal, 30 and -30 degree pose variation and occlusion variability. To create metadata of images, researchers were manually

Fig. 3 Sample Images from UBIPr Database

annotated the images for iris center, canthus points and inner, outer, mid points of eyebrow. Annotations also included information about gaze angle, gender, pigmentation level, eye closure and presence of glasses. Sample images from UBIPr database is shown in Fig. 3.

3.2 Proposed ROI extraction algorithms

The core objective of this research is to identify an optimal size periocular ROI for authentication when subject is wearing face mask. From the literature review, it is found that most of the existing ROI extraction algorithms [2, 14, 19, 21] extracts rectangular ROIs and use some multiplication factors which needs to be calculated empirically in order to calculate the length and breadth of the rectangular ROI. Thus, the objective was to find a ROI extraction method without using any multiplication factors and dynamically adaptive to each person's periocular region. For this, some experiments have been performed by extracting different ROIs on images with masks. It is found that feature enriched region around the eye should include four critical features of periocular region i.e. canthus point, eye socket, shape of eyebrow and eye shape. Considering the above fact, this research proposes two different shapes of ROIs - rectangular and polygon covering all the four critical features in the visible region when most of the face area is occluded because of face mask. Example images to illustrate both the ROIs are shown in Fig. 4.

3.2.1 Rectangular shaped ROI extraction and matching

The objective was to identify a rectangular shaped ROI which includes four critical features of periocular region i.e. canthus point, eye socket, shape of eyebrow and eye shape. To find the height of the rectangular ROI, the distance between the midpoint of the line connecting the canthus points and the midpoint of the eyebrows calculated and it is marked as d in Fig 5. By visualizing the symmetry of the eye shape, it has been decided to take a distance d above and a distance d/2

Fig. 4 Illustration of Polygon and Rectangular ROI

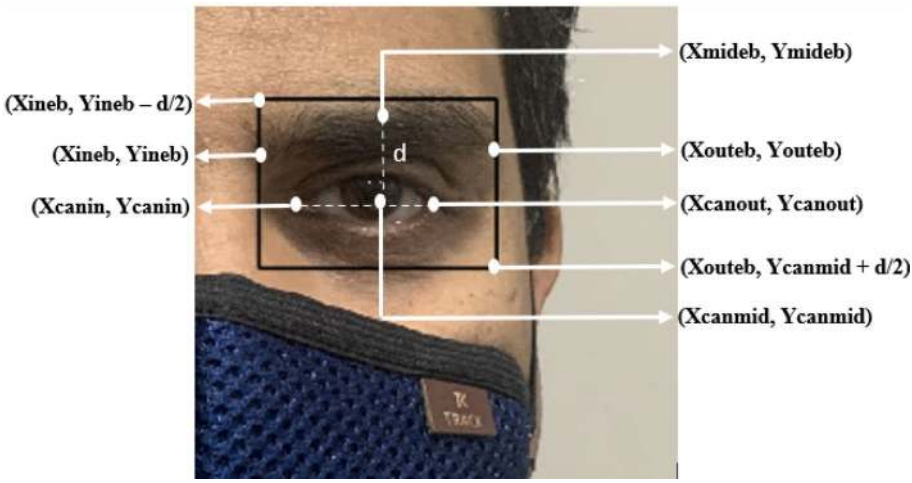

Fig. 5 Illustration of rectangular ROI extraction method

below the midpoint of the line connecting the canthus points as the height of the ROI. Then for the breadth of the rectangular ROI the distance between the eyebrow endpoints are calculated.

The rectangular ROI extraction algorithm uses the end points and midpoints of eyebrow and canthus points as reference points and is given in algorithm 1.

Algorithm 1: Rectangular shaped ROI extraction

Input: Periocular image and following reference points
(X_{outeb}, Y_{outeb}): coordinates of outer eyebrow points
(X_{ineb}, Y_{ineb}): coordinates of inner eyebrow points
(X_{mideb}, Y_{mideb}): coordinates of midpoint of eyebrow
(X_{canin}, Y_{canin}): coordinates of inner canthus point
(X_{canout}, Y_{canout}): coordinates of outer canthus point

Output: Rectangular ROI extracted from periocular images

Step 1: Calculate the midpoint coordinates of the line drawn between inner and outer canthus point

$$x_{canmid} = (x_{canin} + x_{canout})/2 \quad (1)$$
$$y_{canmid} = (y_{canin} + y_{canout})/2 \quad (2)$$

Step 2: Calculate the distance between the midpoint of the eyebrow (X_{mideb}, Y_{mideb}) and obtained coordinates point from step 1 (X_{canmid}, Y_{canmid}) Let it be 'd'.

$$\mathrm{d} = \sqrt{(X_{mideb} - X_{canmid})^2 + (Y_{mideb} - Y_{canmid})^2} \quad (3)$$

Step 3: Calculate the top left (X_1, Y_1) and bottom right (X_2, Y_2) vertices of rectangle

For Right Eye

$$topleft(X_1, Y_1) = (X_{ineb}, Y_{ineb} - d/2) \quad (4)$$
$$bottomright(X_2, Y_2) = (X_{inouteb}, Y_{canmid} + d/2) \quad (5)$$

For Left Eye

$$topleft(X_1, Y_1) = (X_{outeb}, Y_{outeb} - d/2) \quad (6)$$
$$bottomright(X_2, Y_2) = (X_{ineb}, Y_{canmid} + d/2) \quad (7)$$

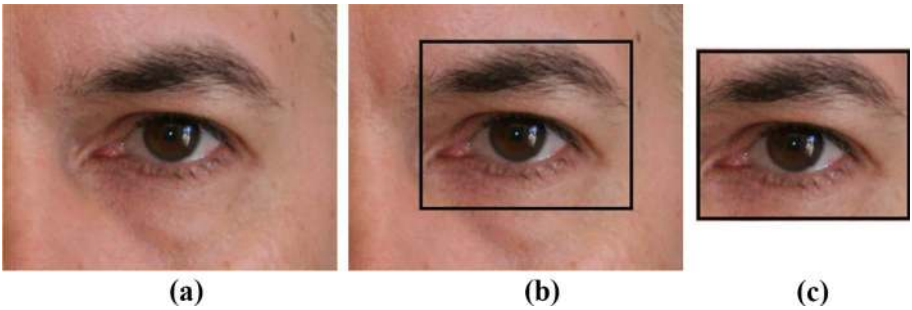

Fig. 6 Example image: (**a**) Original Image (**b**)Visualization of Rectangular ROI (**c**) Cropped Rectangular ROI

An example image after extracting rectangular ROI from UBIPr database is shown in Fig. 6

3.2.2 Polygon shaped ROI extraction and matching

This research also proposes a polygon shaped ROI which is smaller in size than the rectangular ROI yet includes the four critical features of periocular region i.e. canthus point, eye socket, shape of eyebrow and eye shape. This polygon shaped ROI may be useful in situations where the face is highly occluded because of mask or because of some specific hair styles (such as Pixie cut) as shown in Fig. 7.

The height of the proposed polygon ROI will be same as that of the rectangular ROI and the width of the upper side of the polygon is the distance between the eyebrow end points and the lower side is the distance between the canthus points. The construction of polygon shaped ROI is shown in Fig. 8.

Fig. 7 Example image where polygon ROI is more useful as compare to rectangular ROI (**a**) highly occluded face because of face mask (**b**) occlusion because of hair style

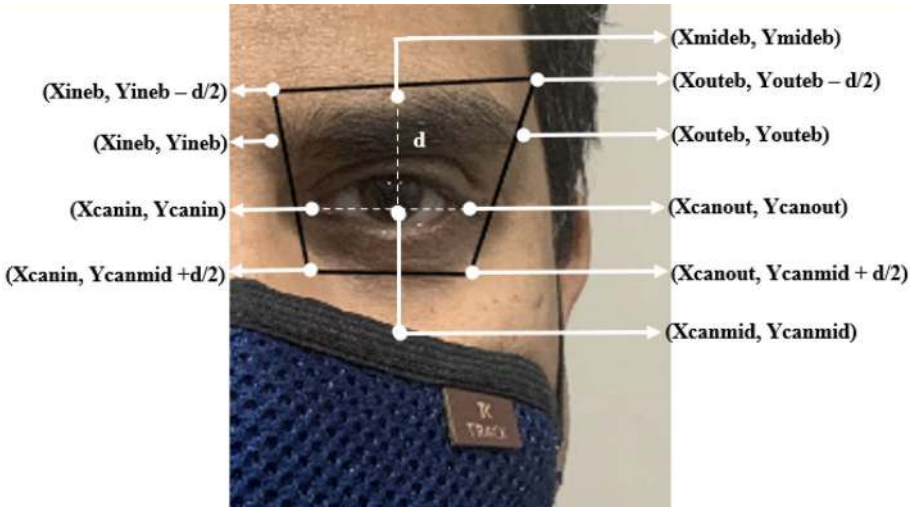

Fig. 8 Illustration of Polygon ROI extraction method

The polygon ROI extraction algorithm also uses the end points and midpoints of eyebrow and canthus points as reference points and is given in algorithm 2.

Algorithm2: Polygon shaped ROI extraction

Input: Periocular image and the following reference points
(X_{outeb}, Y_{outeb}): coordinates of outer eyebrow points
(X_{ineb}, Y_{ineb}): coordinates of inner eyebrow points
(X_{mideb}, Y_{mideb}): coordinates of midpoint of eyebrow
(X_{canin}, Y_{canin}): coordinates of inner canthus point
(X_{canout}, Y_{canout}): coordinates of outer canthus point

Output: Polygon ROI extracted from periocular images

Step 1: Calculate the coordinates of the midpoint of the line connecting the inner and outer canthus points as given in equation 1 and equation 2 call them (X_{canmid}, Y_{canmid}).

Step 2: Calculate the distance between the midpoint of the eyebrow (X_{mideb}, Y_{mideb}) and (X_{canmid}, Y_{canmid}) as shown in equation 3. Let it be 'd'.

Step 3: Calculate the four vertices of polygon as,

For Right Eye

$$(X_1, Y_1) = (X_{ineb}, Y_{ineb} - d/2) \quad (8)$$

$$(X_2, Y_2) = (X_{canin}, Y_{canmid} + d/2) \quad (9)$$

$$(X_3, Y_3) = (X_{canout}, Y_{canmid} + d/2) \quad (10)$$

$$(X_4, Y_4) = (X_{outeb}, Y_{outeb} - d/2) \quad (11)$$

For Left Eye

$$(X_1, Y_1) = (X_{outeb}, Y_{outeb} - d/2) \quad (12)$$

$$(X_2, Y_2) = (X_{canout}, Y_{canmid} + d/2) \quad (13)$$

$$(X_3, Y_3) = (X_{canin}, Y_{canmid} + d/2) \quad (14)$$

$$(X_4, Y_4) = (X_{ineb}, Y_{ineb} - d/2) \quad (15)$$

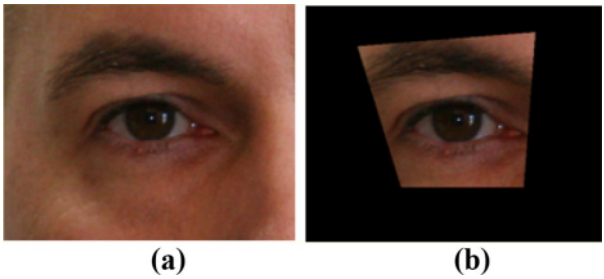

Fig. 9 Example images: (**a**) Original Image (**b**)Polygon ROI

An example image after masking the region outside polygon ROI from UBIPr database is shown in Fig. 9.

3.3 Methodology used

The complete methodology used for ROI extraction, feature extraction from ROI and classification is shown in Fig. 10 and Fig. 11

In the proposed methodology, deep CNN models are used for feature extraction and classification and is described in Sect. 3.5 and Sect. 3.6. The input to the CNN model is the image corresponds to the extracted ROI. For the rectangular ROI, no further processing is required but the polygon ROI need to be converted into an image and the method is described in Sect. 3.3.1.

3.3.1 Extraction of RGB pixel values from polygon region and creation of input image to feed them in to CNN

In order to convert the polygon shaped ROI into an image suitable for inputting the CNN, a row-wise pixel scan (raster scan) has been performed on the images with masked polygon ROI region. The masking process simply converts all the three - Red, Green and Blue channel value of an image pixel to zero. Hence in order to extract the pixels from the polygon ROI, it is enough to extract only those pixels for which the value of any of the three channels (Red, Blue and Green) is not zero. After complete scan of the image, the obtained pixels are stored in a 3-dimensional matrix. This 3D matrix is converted to .jpeg image.

3.4 Proposed CNN architecture for feature extraction and classification

By considering the popularity of non-handcrafted features and to analyse the performance of proposed polygon and rectangular shaped ROI, a deep CNN model has been designed.

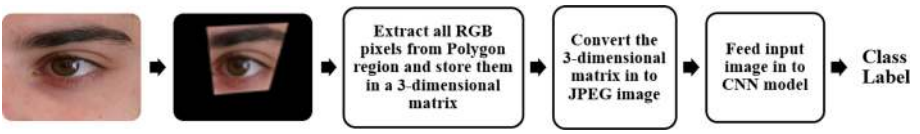

Fig. 10 Proposed Methodology (Polygon ROI extraction and matching)

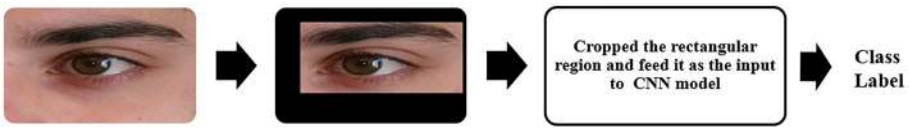

Fig. 11 Proposed Methodology (Rectangular ROI extraction and matching)

The proposed model contains three residual connections and five convolutional layers. Each convolution layer is followed by one ReLU layer. It is followed by a Fully connected layer, a SoftMax layer and finally the Classification layer as shown in Fig. 12.

Here, convolution layers are used to extract features by applying filters on images, ReLU layer maps all the negative values to zero, residual connections are used for optimal gradient flow. The output of the whole process is feed in to fully connected layer. Fully connected layer with SoftMax and Classification layer is used for classification and to predict the best class label for input test images. The description of five subsequent convolutional layers are as follows:

1. First two Convolutional layers (Conv 1 and Conv 2) contains 16 filters of size 5×5 with stride of two pixels.
2. Rest of the three Convolutional layers (Conv 3, Conv 4 and Conv 5) contains 16 filters of size 3×3 with stride of two pixels.

3.5 VGG19 CNN model and transfer learning

An off the shelf pretrained deep CNN model (VGG19) with transfer learning approach is also implemented to analyse the effectiveness of both rectangular and polygon shaped ROIs. Transfer learning approach aims to transfer knowledge (features, weight etc.) from previously learned tasks to newer task, when training samples for the newer task are insufficient to train a robust model [10]. In image classification, transfer learning is used to create a bridge between source feature space to target feature space using a translator in order to transfer the learning from source to target. In this study, we have implemented transfer learning on pre-trained deep CNN VGG19 model by freezing initial ten layers of the pre-trained model. Freezing means, while backward pass the weights on these layers will not

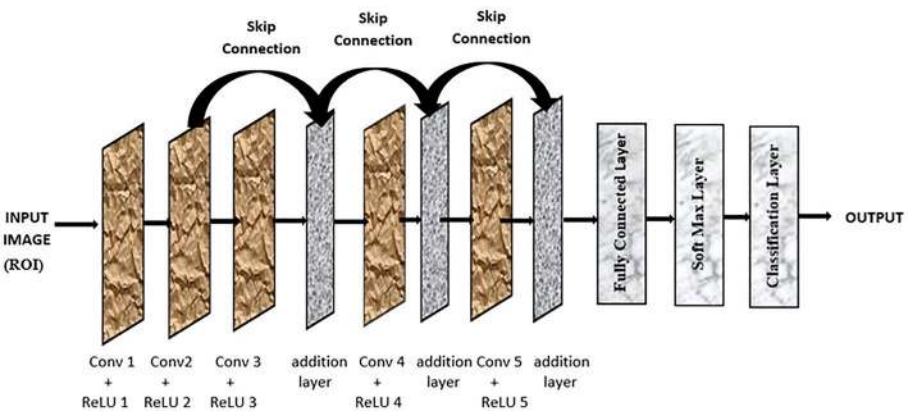

Fig. 12 Architecture of the proposed CNN model

Table 1 Parameter Description

Parameter	Value (for proposed CNN architecture)	Value (for VGG19 architecture)
Learning Algorithm	Root Mean Square Propagation (RMSprop)	Stochastic Gradient Descent with Momentum (SGDM)
Momentum	0.9000	0.9000
Learning Rate	0.0008	0.0001
Weight factor	10	10
Bias factor	10	10
L2 regularization	1.0000e-04	1.0000e-04
Gradient threshold method	'l2norm'	'l2norm'
No of Epochs	6	8
Mini Batch size	16	4

be updated. The weights are the values which will transfer to some new task. The end layers were replaced or fine-tuned based on the new classification task.

VGG19 deep CNN model consists of 19 layers with trainable weights. It includes 16 convolutional layer and 3 fully connected layer apart from that it consists of 5 max pooling layer which is used to reduce the size of the input and a soft max layer which is used to take final decision about prediction.

4 Experiments

All experiments were carried out using the MATLAB r2018b on a system with Intel Core i7-8750H GPU Processor @ 2.2 GHZ, 8GB DDR4 RAM with windows 10 operating system. Performance of both the ROIs (polygon and rectangle) extracted using the proposed algorithms were analyzed with two different CNN classifier models described in Sect. 3.4 and Sect. 3.5. After evaluating a lot of different set of hyper parameters such as different learning rates (0.0001, 0.0003, 0.0005 and 0.0008), minibatch size (2, 4, 8, 16, 32) and epoch (starting from 2 to 10), the final parameter specification used to train the proposed CNN model and VGG19 model is shown in Table 1.

Three different experiments were carried out to evaluate the performance of both the ROIs (polygon and rectangle) extracted using the proposed algorithms.

Experiment 1: Complete UBIPr database

In this experiment, complete UBIPr dataset is utilized and divided it into training, validation and test set. The partition is based on the Pareto principal- Pareto Principal suggest to divide dataset in to 80: 20 ratios. 80% of the images from all 344 subjects are selected randomly and kept for training and validation set and the remaining 20 % are kept for testing set. From training and validation set, again 80 % of the images are randomly selected to train the model and remaining 20% are used for validating the model. Details for number of images used for training, validation and testing are shown in Table 2.

Table 2 Dataset Statistics for Experiment 1

Database Name	Training Dataset	Validation Dataset	Test Dataset
UBIPr	6025	1152	3075

Table 3 Dataset Statistics for Experiment 2

Database Name	Training Dataset	Validation Dataset	Test Dataset
UBIPr	3000 (with 0 degree pose variation)	1252	3000 (30 degree pose variation) 3000 (-30 degree pose variation)

Experiment 2: Images with pose variation

In this experiment to analyse the effectiveness of both the extracted ROIs, a non -ideal scenario in which images suffered with pose variation (30 and -30 degree) were used for testing. Both the models were trained using frontal images (0 degree pose variation) only. Details of number of images used in training as well as testing of both the model is shown in Table 3. Both the proposed CNN and VGG19 architecture were used for testing the performance of the ROIs in recognition.

Experiment 3: Subject are wearing glasses

In this experiment, one more non-ideal scenario in which testing dataset contains only those images of subjects wearing glasses were also used to analyse the performance of both the extracted ROIs. Details of number of images used for training as well as testing of both the models is shown in Table 4. Both the proposed CNN and VGG19 architecture were used for testing the performance of the ROIs in recognition.

5 Result and discussion

The key innovation of this study is the identification of optimum size periocular region of interest for biometric authentication when subject is wearing face mask. Thorough analysis has been performed to analyze the efficiency of the proposed polygon and rectangular shaped periocular ROI from different perspectives such as the performance of both the ROIs in two different non-ideal scenarios when images are suffered with pose variation and when subjects are wearing glasses, training time taken by both the models and size of ROIs.

5.1 Recognition accuracy

To analyse the performance of both polygon and rectangular shape ROI using two different CNN architecture (proposed CNN and VGG19) this study implemented closed identification system scenario and used Rank 1 recognition accuracy as performance metrics.

$$Rank\ 1\ Recognition\ Accuracy = \frac{total\ number\ of\ predicted\ class\ label\ those\ are\ correctly\ predicted}{total\ number\ of\ class\ label} \times 100 \qquad (16)$$

The Rank 1 accuracy calculated for both polygon and rectangular ROI extracted from UBIPr database using both proposed CNN and VGG19 model in Experiment 1,

Table 4 Dataset Statistics for Experiment 3

Database Name	Training Dataset	Validation Dataset	Test Dataset
UBIPr	7527	1720	1005

Experiment 2 and Experiment 3 are shown in Tables 5, 6 and 7 respectively whereas comparison of Rank 1 to Rank 10 recognition accuracy using CMC curve is illustrated in Figs. 13, 14 and 15 respectively.

5.2 Training time

The total training time taken by the proposed CNN architecture and pretrained CNN model for both polygon and rectangular shape ROI for complete UBIPr database is shown in Table 8.

It is observed that training time taken by the proposed CNN is much less compared to VGG19 also the training time taken by both CNN models with polygon ROI is less compared to rectangular ROI even though it is marginal. It may be due to the smaller number of features in polygon ROI compared to rectangular ROI.

5.3 Size of ROI

A comparative analysis for the size of polygon and rectangular ROI in terms of number of pixels they contain is done with reference to a selected image and is shown in Table 9.

It is observed that number of pixels contained in polygon ROI is around 39 % less as compared to rectangular ROI and still has all necessary features to obtain acceptable recognition accuracy.

5.4 Comparison with pre-existing work in literature

The proposed approach is also compared with the state-of-the-art works on complete UBIPr database. The comparison results clearly show an improvement in recognition accuracy as shown in Table 10.

Based on the experiments on UBIPr database using both polygon and rectangular shaped ROI, it is observed that both the ROIs performed well with proposed five-layer CNN model and VGG19 model. Moreover Experiment 2 and Experiment 3 shows the effectiveness of proposed ROIs in non-ideal scenarios when the test dataset contains images with pose variation and when subjects are wearing glasses.

The proposed rectangular ROI region is 18% to 20% less in area compared to the rectangular ROI used in our previous work [12], but still performs better. This shows that the ROI extracted using the proposed algorithms are feature enriched small regions around both the left and right eye.

Table 5 Rank 1 recognition accuracy (Experiment 1: complete database)

Method	Rank 1 (%) Polygon ROI	Rank 1 (%) Rectangular ROI
Proposed CNN model	82.4	84.5
VGG19 Model	86.3	90

Table 6 Rank 1 recognition accuracy (Experiment 2: images with pose variation)

Method	Rank 1 (%) Polygon ROI		Rank 1 (%) Rectangular ROI	
	30 deg	**-30 deg**	**30 deg**	**-30 deg**
Proposed CNN model	86.8	88	90	91.8
VGG19 Model	94	94	94.2	96

Table 7 Rank 1 recognition accuracy (Experiment 3: subjects wearing glasses)

Method	Rank 1 (%) Polygon ROI	Rank 1 (%) Rectangular ROI
Proposed CNN model	90	94.5
VGG19 Model	95.2	98.5

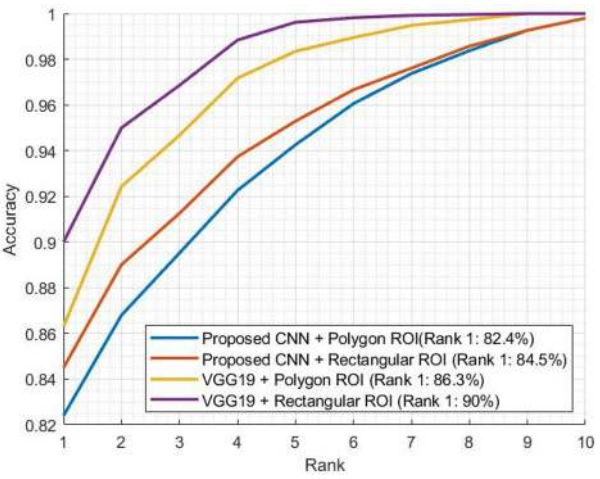

Fig. 13 CMC curve (complete database): Proposed CNN + Polygon ROI vs Proposed CNN + Rectangular ROI vs VGG 19 + Polygon ROI vs VGG19 + Rectangular ROI on UBIPr database

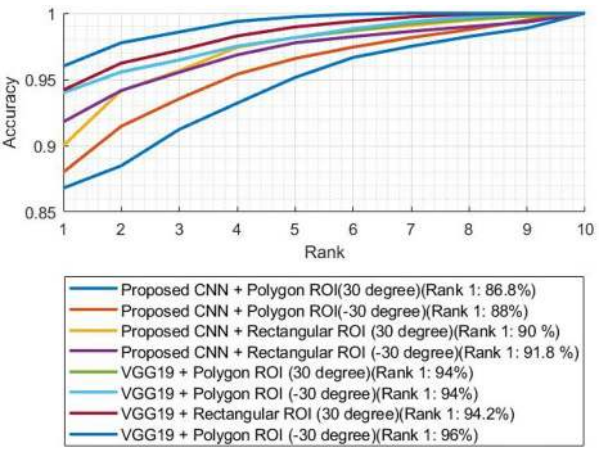

Fig. 14 CMC curve (pose variation): Proposed CNN + Polygon ROI vs Proposed CNN + Rectangular ROI vs VGG 19 + Polygon ROI vs VGG19 + Rectangular ROI on UBIPr database

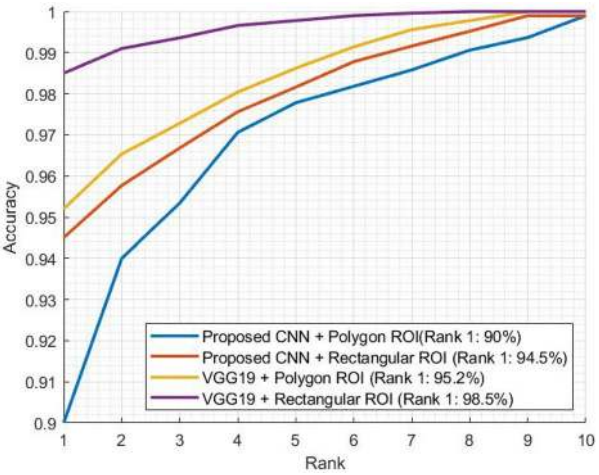

Fig. 15 CMC curve (subject wearing glasses): Proposed CNN + Polygon ROI vs Proposed CNN + Rectangular ROI vs VGG 19 + Polygon ROI vs VGG19 + Rectangular ROI on UBIPr database

Table 8 Training time

Method	Training Time Polygon ROI	Training Time Rectangular ROI
Proposed CNN model	4 min 14 s	4 min 35 s
VGG19 Model	111 min 16 s	114 min 12 s

Table 9 Size of ROI

Shape of the ROI	Number of pixels
Polygon Shape	1578
Rectangular Shape	4096

Table 10 Comparison with pre-existing approaches

References	Database	Methodology	Rank1 Acc (%)
Proposed approach	UBIPr	Polygon ROI + VGG 19	86.3
		Rectangular ROI + VGG 19	90
[12]	UBIPr	Rectangular ROI + VGG 19	89.50
[24]	UBIPr	Rectangular ROI + Rotation Invariant Uniform LBP	85.7
[26]	UBIPr	Rectangular ROI + Patch similarity score	L: 84.14, R: 78.59
[17]	UBIPr	Rectangular ROI + CRBM with Dense SIFT	50.1

**LBP* Local Binary Pattern, *CRBM* Convolutional Restricted Boltz man Machine, *SIFT* Scale Invariant Feature Transform, *L* Left eye, *R* Right Eye

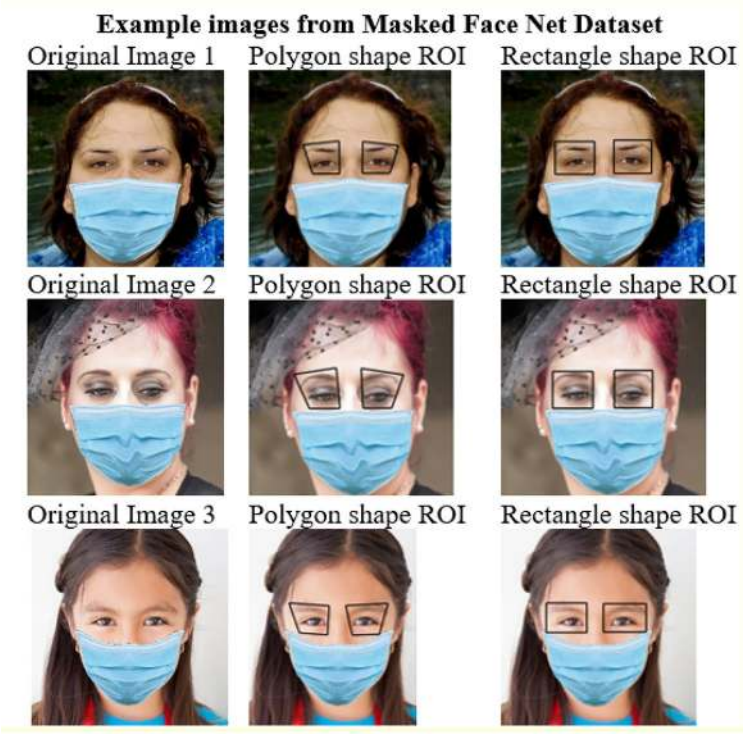
Example images from Masked Face Net Dataset
Original Image 1
Polygon shape ROI
Rectangle shape ROI
Original Image 2
Polygon shape ROI
Rectangle shape ROI
Original Image 3
Polygon shape ROI
Rectangle shape ROI

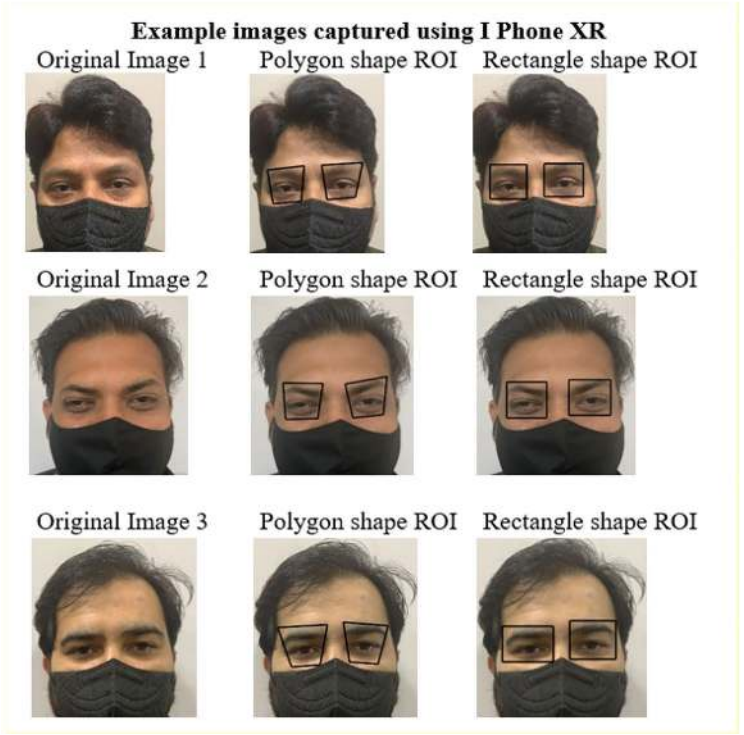
Example images captured using I Phone XR
Original Image 1
Polygon shape ROI
Rectangle shape ROI
Original Image 2
Polygon shape ROI
Rectangle shape ROI
Original Image 3
Polygon shape ROI
Rectangle shape ROI

◂**Fig. 16** Illustration of polygon and rectangular ROI on images with masks

5.5 Illustration of generalization capability of proposed algorithms to extract polygon and rectangular ROI

To examine the generalizability of the proposed algorithms for ROI extraction, we have applied both the ROI extraction algorithms on different images randomly chosen from publicly available Masked Face Net Dataset [5] as well as on images captured using mobile phone camera. Some of the images illustrating both polygon and rectangular ROI are shown in Fig. 16.

Here, the first three images were randomly chosen from MASKED FACENET DATASET, and last three images were captured in real time using I phone XR having 12-megapixel camera with an f/1.8 aperture in a controlled environment. From Fig. 16, It is observed that the proposed ROI are within the visible region when subjects are wearing different types of face masks contains all the required critical features within that small ROI.

6 Conclusion and future work

Human beings are presently confronting the covid-19 global pandemic which has shaken the whole world. With lots of worries, this situation is giving us an opportunity to think out of the box to develop strategies and tactics to mitigate its effects. Indeed, the digital technology in every domain needs to be upgraded. This paper deals with the problem of occlusion, caused by face mask in the biometric systems. As a solution, this research proposes algorithms to extract different shape (polygon and rectangular) ROIs from the visible periocular region when subjects are wearing masks. The proposed algorithms use five reference points (inner canthus point, outer canthus point, end points and midpoint of eyebrow) in order to include the complete shape of the periocular region of the individual. End point of eyebrows ensures the inclusion of complete eyebrow shape and canthus point ensures the inclusion of eye shape of the individual in the proposed ROIs.

The proposed rectangular ROI shows marginal improvement in recognition accuracy compared with the polygon shaped ROI due to larger area and thus more features. However, the polygon ROI may be useful when the subject's face is highly occluded due to face mask or hair.

This paper also proposes a simple five convolutional layer CNN model with residual connections for evaluating the performance of the proposed ROIs. The pretrained VGG19 CNN model is also used for evaluation and it is found that the training time taken by the proposed CNN model is much less compared to VGG19, yet gives comparable recognition accuracy. The performance of the proposed method is also compared with the state-of-the-art rectangular ROI based methods and the experimental results provide very strong support to the proposed ROIs which are unique of its type and to the best of our knowledge nothing like this is proposed by anyone in the area of periocular biometrics for subject identification when half of the nose area is covered with the face mask.

In future, we are aiming to reduce the number of reference points required to extract optimal size periocular ROIs in order to reduce the complexity of ROI extraction algorithms.

Funding This research did not receive any specific grant from funding agencies in the public, commercial, or not-for-profit sectors.

Declarations

Competing interests The authors have no relevant financial or non-financial interests to disclose.

References

1. Agarwal S, Punn NS, Sonbhadra SK, Nagabhushan P, Pandian KK, Saxena (2019) Unleashing the power of disruptive and emerging technologies amid COVID 2019: A detailed review. https://arxiv.org/abs/2005.11507
2. Ahmed NU, Cvetkovic S, Siddiqi EH, Nikiforov A, Nikiforov I (2017) Combining iris and periocular biometric for matching visible spectrum eye images. Pattern Recogn Lett 91:11–16. https://doi.org/10.1016/j.patrec.2017.03.003
3. Bakshi S, Sa PK, Majhi B (2013) Optimized periocular template selection for human recognition. Biomed Res Int. https://doi.org/10.1155/2013/481431
4. Bharadwaj S, Bhatt HS, Vatsa M, Singh R (2010) Periocular biometrics: When iris recognition fails. Proc 4th IEEE Int Conf on Biometrics: Theory, App Syst (BTAS), Washington, DC, USA, 1–6. https://doi.org/10.1109/BTAS.2010.5634498
5. Cabani A, Hammoudi K, Benhabiles H, Melkemi M (2020) MaskedFace-Net–A dataset of correctly/incorrectly masked face images in the context of COVID-19. Smart Health 19:100144. https://doi.org/10.1016/j.smhl.2020.100144
6. Castrillón-Santana M, Lorenzo-Navarro J, Ramón-Balmaseda E (2016) On using periocular biometric for gender classification in the wild. Pattern Recogn Lett 82(2):181–189. https://doi.org/10.1109/TPAMI.2009.155
7. Damer N, Grebe JH, Chen C, Boutros F, Kirchbuchner F, Kuijper A (2020) The effect of wearing a mask on face recognition performance: an exploratory study. Proc IEEE Int Conf of the Biometrics Special Interest Group (BIOSIG), Darmstadt, Germany,1–6
8. Dong Y, Woodard DL (2011) Eyebrow shape-based features for biometric recognition and gender classification: A feasibility study. International Joint Conference on Biometrics, Washington, DC, USA. 1–8. https://doi.org/10.1109/IJCB.2011.6117511
9. Geva Fii Co-CEO Gur (2020) Face ID firms battle Covid-19 as users shun fingerprinting. https://doi.org/10.1016/S0969-4765(20)30042-4. Accessed 23 Sept 2020
10. Hussain M, Bird JJ, Faria DR (2018) A Study on CNN Transfer Learning for Image Classification, Workshop on Computational Intelligence, Nottingham, Springer, 191–202. https://doi.org/10.1007/978-3-319-97982-3_16
11. Keshari R, Ghosh S, Agarwal A, et al. (2016) Mobile periocular matching with pre-Post cataract surgery, Pro IEEE Int Conf on Image Processing, Phoenix, AZ, USA. 1–6. https://doi.org/10.1109/IJCB.2016.7532933
12. Kumari P, Seeja KR (2019) Periocular Biometrics for Non-ideal Images Using Deep Convolutional Neural Networks. Proc Int Conf on Intelligent Computing and Communication, Bangalore, India, 143–151 https://doi.org/10.1007/978-981-15-1084-7_15
13. Le TH, Prabhu U, Savvides M (2014) A novel eyebrow segmentation and eyebrow shape-based identification. Proc IEEE Int Joint Conference on Biometrics, Clearwater, FL, USA, 1–8. https://doi.org/10.1109/BTAS.2014.6996262
14. Liu P, Jing-Ming Guo J-M et al (2017) Ocular Recognition for Blinking Eyes. IEEE Trans Image Process 26(10):5070–5081. https://doi.org/10.1109/TIP.2017.2713041
15. Mahalingam G, Ricanek K, Albert AM (2014) Investigating the periocular-based face recognition across gender transformation. IEEE Trans Inf Forensics Secur 9(12):2180–2192. https://doi.org/10.1109/TIFS.2014.2361479
16. Nguyen HM, Rattani A, Derakhshani R (2020) Eyebrow Deserves Attention: Upper Periocular Biometrics. Proc IEEE Int Conf of the Biometrics Special Interest Group (BIOSIG), Darmstadt, Germany,1–5
17. Nie L, Kumar A, Zhan S (2014) Periocular recognition using unsupervised convolutional RBM feature learning. Proc Int Conf on Pattern Recognition, Stockholm, Sweden 399–404. https://doi.org/10.1109/ICPR.2014.77

18. Okereafor K, Ekong I, Markson IO, Enwere K (2020) Fingerprint Biometric System Hygiene and the Risk of COVID-19 Transmission, JMIR Biomedical Engineering, 5, (1): 1–37. https://doi.org/10.2196/19623
19. Park U, Ross A, Jain AK (2009) Periocular Biometrics in the Visible Spectrum: A Feasibility Study. Proc 3rd IEEE Int Conf on Biometrics: Theory, App Syst, Washington, DC, USA.153–158. https://doi.org/10.1109/BTAS.2009.5339068
20. Padole CN and Proenca H (2012) Periocular recognition: analysis of performance degradation factors. Proc 5th IAPR Int Conf on biometrics (ICB), New Delhi, India, 439–445. https://doi.org/10.1109/ICB.2012.6199790
21. Park U, Jillela R, Ross A (2010) Jain AK (2010) Periocular biometrics in the visible spectrum. IEEE Trans Inf Forensics Secur 6(1):96–106. https://doi.org/10.1109/TIFS.2010.2096810
22. Proença H, Neves JC, Santos G (2014) Segmenting the periocular region using a hierarchical graphical model fed by texture/shape information and geometrical constraints. Proc. IEEE Int. Joint Conf. on Biometrics, Clearwater, FL, USA,1–7. https://doi.org/10.1109/BTAS.2014.6996228
23. Proença H, Neves João C (2018) Deep-PRWIS: Periocular Recognition Without the Iris and Sclera Using Deep Learning Frameworks IEEE Trans Inform Forensics Sec, 13(4): 888–896. https://doi.org/10.1109/TIFS.2017.2771230
24. Raffei A, FM, Sutikno T, Asmuni H, Hassan R, Othman RM, Kasim S, Riyadi MA (2019) Fusion Iris and Periocular Recognitions in Non-Cooperative Environment'. Indonesian J Electric Eng Inform 7(3):543–554. https://doi.org/10.11591/ijeei.v7i3.1147.40
25. Raja KB, Raghavendra R, Stokkenes M, Busch C (2014) Smartphone authentication system using periocular biometrics. Proc IEEE Int Conf of the Biometrics Special Interest Group (BIOSIG), Darmstadt, Germany, 1–8
26. Smereka JM, Kumar BVKV, Rodriguez A (2016) Selecting discriminative regions for periocular verification, Proc Int Conf on Identity, Security and Behaviour Analysis, Sendai, Japan. https://doi.org/10.1109/ISBA.2016.7477247
27. Zhao Z, Kumar A (2018) Improving periocular recognition by explicit attention to critical regions in deep neural network. IEEE Trans Inf Forensics Secur 13(12):1–15. https://doi.org/10.1109/TIFS.2018.2833018